3D SEGMENTATION OF RODENT BRAINS USING DEFORMABLE MODELS AND VARIATIONAL METHODS

Shaoting Zhang, Jinghao Zhou,
Xiaoxu Wang, Sukmoon Chang,
Dimitris N. Metaxas
CBIM, Rutgers University
Piscataway, NJ, USA
shaoting@cs.rutgers.edu
jhzhou@eden.rutgers.edu
dnm@cs.rutgers.edu

George Pappas, Foteini Delis,
Nora D. Volkow, Gene-Jack Wang,
Panayotis K. Thanos
Behavior Neuropharmacology and Neuroimaging Lab,
Medical Department,
Brookhaven National Laboratory
Upton, NY, USA

Chandra Kambhamettu
Computer and Information Sciences,
University of Delaware
Newark, DE, USA

Abstract

3D functional segmentation of brain images is important in understating the relationships between anatomy and mental diseases in brains. Volumetric analysis of various brain structures such as the cerebellum plays a critical role in studying the structural changes in brain regions as a function of development, trauma, or neurodegenerationin. Although various segmentation methods in clinical studies have been proposed, many of them require a priori knowledge about the locations of the structures of interest, which prevents the fully automatic segmentation. Besides, the topological changes of structures are difficult to detect. In this paper, we present a novel method for detecting and locating the brain structures of interest that can be used for the fully automatic 3D functional segmentation of rodent brain MR images. The presented method is based on active shape model (ASM), Metamorph models and variational techniques. It focuses on detecting the topological changes of brain structures based on a novel volume ratio *criteria. The mean successful rate of the topological change detection shows 86.6% accuracy compared to the expert identified ground truth.*

1. Introduction

3D functional segmentation of brain images is important to understand the relationships between anatomy and mental diseases in brains [1]. Volumetric analysis of rodent brain structures, such as the cerebellum, the caudate putamen, the hippocampus, the fibria, the external capsule, the neocortex, the cerebral cortex, the striatum, the septum, the ventricles, and the thalamus plays a critical role in studying the structural changes occurring in specific brain regions as a function of development, trauma or neurodegeneration [2]. Volumetric analysis of gray matter (GM), white matter (WM), and cerebrospinal fluid (CSF) is used to characterize morphological differences between subjects in psychiatric disease including schizophrenia, epilepsy or Alzheimer's disease [3, 4]. Volumetric analysis can also be used to analyze drug addiction and alcoholism [5, 6]

Many semi-automatic and automatic segmentation methods in clinical studies have been proposed since manual segmentation of brain images is time-consuming and lacks the reproducibility due to a large intra- and inter-observer variability. Pitiot et al. developed an expert-knowledge guided segmentation system for anatomical structures in MRI, which uses medical expertise in the form of implicit or explicit knowledge [7]. Leventon et al. presented a method of incorporating shape information into the image segmentation process [8]. Barra and Boire combined medical expertise with fuzzy maps using information fusion to segment anatomical structures in brain MRIs [9]. Niessen et al. presented an MRI brain segmentation method which combines an edge dependent multiscale representation with an intensity based linking scheme [10]. Shen et al. presented an adaptive deformable model for automati-

978-1-4244-3993-5/09/$25.00 ©2009 IEEE

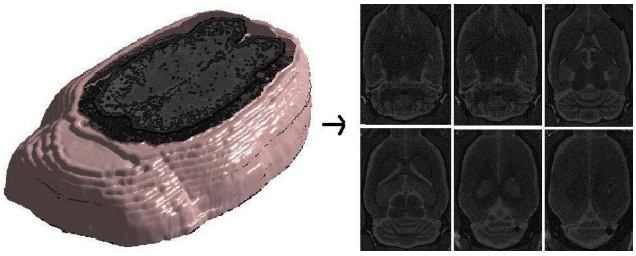

Figure 1. 3D rat brain volume and its unfolded 2D slices.

cally segmenting brain structures from volumetric MR images [11]. Zhou et al. presented a fully automated segmentation method of rodent brain volume by extending the robust active shape models to incorporate an automatic prior shape selection process [12]. In our previous research, we used 2D ASM [13] and Metamorph [14, 15] to segment rodent brains and computed area ratio between two results to predict missing structures [16]. Although these methods generally produce promising results, many of them require a priori knowledge on the existence and the locations of the structures of interest, preventing the fully automatic 3D segmentation.

In this paper, we propose a prediction method for the existence of brain structures, to be used for a fully automatic functional segmentation of 3D rodent brain MRIs. The method focuses on detecting the topological changes of brain structures based on a novel *volume ratio* criteria. The topological changes of brain structures in the context of 3D brain MRI images include missing structures and emerging structures, as can be seen in Fig. 1. The proposed method allows many existing segmentation methods to address the issue of missing or emerging 3D structures of interest.

The proposed method compares the volume ratio between ASM and Metamorph's 3D results to detect topological changes of the brain structures (e.g., missing structures). First ASM is applied on all slices. Between each neighbor slices, corresponding resulting control points are connected and linear interpolated to form a simple volume. Note that this result is only for comparison purpose but not a 3D segmentation. The reason of not using 3D ASM is that it requires many datasets and labels for training purpose. Large datasets and accurate labels from experts are not available in our cases. Thus 2D ASM is chosen, which needs relatively small datasets. After ASM step, Metamorph and variational techniques [17] are applied to do 3D segmentation. Note that Metamorph does not require training data. Two initializations (contours) are automatically placed on the first and last slices. Variational techniques including implicit function and radial basis function (RBF) are employed to generate 3D volume consisting of these two contours. This initial volume is intersected with slices in between. These intersections are used to initialize Metamorph models on those slices. During the deformation of Metamorph, volumes can be generated based on variational techniques. The final volume obtained is the 3D segmentation result when the structure is successfully detected. If a structure is present in an image, both the ASM and the Metamorph model will segment approximately the same volumes, resulting in the ratio of the segmented volumes close to 1. If the structure is missing, ASM produces a mean 3D volume while Metamorph with two initializations results in a smaller one, resulting in the ratio between two volumes of ASM and Metamorph much less than 1.

Although it was specifically developed for the functional segmentation of rat brain structures, the method is generally applicable to any task involving deformable shape analysis of objects that change their topological structures in a given dataset.

The paper is organized as the following. Section 2.1 shows the big picture of our algorithm framework. The rest part of Section 2 explains algorithms such as ASM, Metamorph and volume ratios. Section 3 validates the correct rate of the prediction method and shows 3D segmentation results. Section 4 makes conclusions.

2. Algorithms

2.1. Overview

Our algorithm consists of two pipelines (Fig. 2): ASM and Metamorph. ASM generates a reference volume. Metamorph obtains 3D segmentation result. Using the ration between these two volumes, topological changing can be detected.

In the ASM pipeline, we use the same control points on every slices and roughly generate shapes. By connecting corresponding control points in each neighboring slices and linearly interpolating, a reference volume can be obtained. This result is not 3D segmentation and is only for comparison purpose. In the Metamorph pipeline, two initializations are automatically placed in the first and last slices. Then variational techniques and implicit function are employed to generate 3D volume containing two initializations. The resulting volume intersects with slices in between. These intersections are used as Metamorph's initializations in these slices. During Metamorph's deformation, variational techniques are repeatedly applied to get volume. Finally it generates 3D segmentation result. Comparing the volume ration of the results of Metamorph and ASM, topological changing can be found.

To automatically place the control points or initialization, nonparametric kernel regression is also needed (Section 2.2).

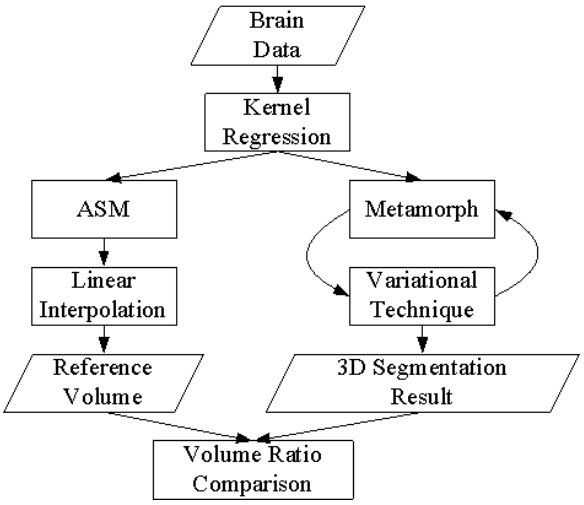

Figure 2. Two pipelines in the algorithm framework: ASM and Metamorph.

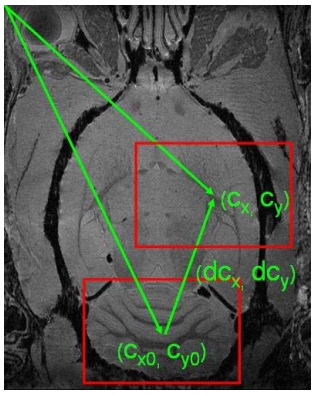

Figure 3. The results of the brain structure detection based on the nonparametric kernel regression.

2.2. Kernel regression

To automatically place control points for ASM and initializations for Metamorph, we need to roughly estimate the position of brain structures. This is called brain structure detection. Nonparametric kernel regression is employed to do this task. Kernel regression is a non-parametric technique to estimate the conditional expectation of a random variable, which can be used to find a non-linear relation between a pair of random variables [18]. The nonparametric kernel regression (NPR) we used is a smoothed k-nearest neighbor (KNN) regression which is an approximation of the conditional mean and an optimal estimate in the L^2 sense. NPR has the following form:

$$f(x) = \frac{\sum_{i=1}^{N} g_\sigma(x; x_i) y(x_i)}{\sum_{i=1}^{N} g_\sigma(x; x_i)} \quad (1)$$

where $g_\sigma(x; x_i)$ is a kernel function. The most widely used kernel function is the Gaussian Radial basis function (GRBF):

$$g_\sigma(x; x_i) = \exp\left(-\frac{\|x - x_i\|^2}{2\sigma^2}\right) \quad (2)$$

The advantage of the GRBF kernel has the noncompact support property. Other kernel functions with compact supports such as the Epanechnikov kernel can also be applied.

Fig. 3 shows the basic idea of the regression-based brain structure detection. We are interested in finding the center position (c_{x_0}, c_{y_0}) of the Cerebellum, assuming that the orientation of the brain is upright and the scale and size of the brain is aligned. During the running time, given an image patch $I(c_x, c_y)$ with its center at (c_x, c_y), the nonparametric kernel regression function estimates the difference vector (d_{c_x}, d_{c_y}) between the current position (c_x, c_y) and the target position (c_{x_0}, c_{y_0}). In other words, the nonparametric kernel regression function gives a mapping $T : I(c_x, c_y) \rightarrow (d_{c_x}, d_{c_y})$. The detail of the method can be found in this paper [19].

2.3. Robust ASM

After detecting the brain structures, control points for robust ASM (RASM) are placed in every slices to generate reference shapes. Neighboring shapes are connected using simple linear interpolation to get a reference volume.

ASM represents the features of a shape as the point distribution model (PDM) [13]. Given a set of training images, the feature of interest in each image is manually labeled with n landmark points and represented as a vector in $2n$-dimensional space, $x =< x_0, y_0, x_1, y_1, ..., x_{n-1}, y_{n-1} >$. After aligning these vectors into a common coordinate system, a set of orthogonal bases P is computed with the principal component analysis. Then, each aligned shape can be reconstructed as $x = \bar{x} + Pb$, where $\bar{x}$ and b are the mean shape and the shape parameter vector, respectively. This model also allows us to search for a new example of the shape in an unlabeled image by varying b appropriately, often based on low-level image features such as the gradients along normal directions to the boundary of an initial shape toward the strongest edge in the image. Although it has been used successfully in many applications, ASM has two important limitations for the segmentation of brain structures in MRI.

The major drawback of ASM for searching for a new example of the shape in an unlabeled image is the initialization of the model. First, if the model is initialized too far from the feature of interest, the process may fail. Second, we usually have multiple structures to be segmented in medical images. If one ASM consisted of several sub-shape models

is initialized on the multiple structures to be segmented, the sub-shape models may be initialized too far from the corresponding features of interest due to the large discrepancies of the structure positions among different brains. To automate the accurate initialization of the model, we use multiple ASMs instead of one composite ASM containing various brain structures. The multiple ASMs incorporate prior knowledge of the positions of different brain structures obtained from the brain structure detection method.

Another limitation of ASM in finding an object in unlabeled images is that it heavily relies on the low-level image features to guide the search for the optimal positions of the feature points. For example, the gradient descent search on the image intensity profile has been widely used to move the model points toward the strongest edge in the image [13]. However, this approach is not suitable for the accurate delineation of Cerebellum of the brain in MRI since Cerebellum is intensity non-uniformity with stripes occlude structures and appear as the strongest edge (Fig. 1). We overcome this difficulty by introducing a robust error function based on the M-estimator [20].

Given an orthogonal basis P obtained from ASM, the projection C of a new example shape X is given by $C = P^T dX$, where $X = \bar{X} + dX$ and $\bar{X}$ is the mean shape of the aligned shapes from the training images. Using the projection C, we can also find a corresponding shape as $\hat{X} = \bar{X} + PC$, in which $\hat{X}$ and PC approximates X and dX , respectively. Therefore, instead of obtaining X by optimizing dX using low-level image features only, our goal is to find the optimal C by minimizing the following robust energy function:

$$E_{rpca}(C) = \rho(\|dX - PC\|, \sigma) \tag{3}$$

where, $\rho(x, \sigma) = x^2/(x^2 + \sigma^2)$ is the Geman-McClure error function and σ is a scale parameter that controls the convexity of the robust function. With an iterative gradient descent search on E, we get:

$$C^{(n+1)} = C^{(n)} + \lambda \Delta C \tag{4}$$

where, λ is a small constant that determines the step size and

$$\Delta C = \frac{\partial E_{rpca}}{\partial C} = -2P(dX - PC)\frac{\sigma^2}{(\|dX - PC\|^2 + \sigma^2)^2} \tag{5}$$

By continuing the iterative process until $\left\|E^{(n+1)} - E^{(n)}\right\| < \varepsilon$, where ε is a preselected tolerance, we obtain the optimal project C and a robust shape in the shape space as:

$$\hat{X} = \bar{X} + PC \tag{6}$$

The 2D results of this process are illustrated in Fig. 4(red contour), where the Cerebellum occluded by the strips are accurately segmented.

2.4. 3D Metamorph

Metamorph is a new class of deformable models, which combine the best features of parametric and geometric models, and introduce novel modeling strategies that unify the representation and deformation schemes for shape and intensity. Detailed description can be found at [15]. Traditional Metamorph works on 2D images. With initializations manually placed by user, the model will deform and hence find the boundary of region-of-interest. For 3D segmentation, user needs to place initializations on every slices and then reconstruct volume from 2D results. In our algorithm, we only need two initializations and generate 3D result automatically. This algorithm consists of traditional Metamorph and variational techniques.

Based on the results of nonparametric kernel regression, two initializations (2D contours) are automatically placed in the first and last slices. These 2D contours can be viewed as scatted data. Variational techniques such as thin-plate spline is applied on the scatted data to get 3D shape [17]. This technique is defined as the variational solution of the following energy function E:

$$E = \int_{\Omega} f_{xx}^2(x) + 2f_{xy}^2(x) + f_{yy}^2(x) \tag{7}$$

Equation 7 can be solved using weighted sums of the radial basis function $\phi = |x|^2 log(|x|)$. Thus we can represent 3D space points as the following implicit function:

$$f(x) = \sum_{j=1}^{n} d_j \phi(x - c_j) + P(x) \tag{8}$$

Where c_j are contour points, d_j are the weights, and $P(x)$ is a degree one polynomial. x can be viewed as 2D coordinates, and $f(x)$ represents the height value. With weight d_j, all points on 3D shape can be obtained by solving Formula 8. d_j is calculated from constraints on two initializations.

$$h_i = \sum_{j=1}^{k} d_j \phi(c_i - c_j) + P(c_i) \tag{9}$$

Using all points on the initializations, and let $c_i = (c_i^x, c_i^y, c_i^z)$, $\phi_{ij} = \phi(c_i - c_j)$, we can write down the following linear system [17]:

$$\begin{bmatrix} \phi_{11} & \phi_{12} & \dots & \phi_{1k} & 1 & c_1^x & c_1^y & c_1^z \\ \phi_{21} & \phi_{22} & \dots & \phi_{2k} & 1 & c_2^x & c_2^y & c_2^z \\ \vdots & \vdots & & \vdots & \vdots & \vdots & \vdots & \vdots \\ \phi_{k1} & \phi_{k2} & \dots & \phi_{kk} & 1 & c_k^x & c_k^y & c_k^z \\ 1 & 1 & \dots & 1 & 0 & 0 & 0 & 0 \\ c_1^x & c_2^x & \dots & c_k^x & 0 & 0 & 0 & 0 \\ c_1^y & c_2^y & \dots & c_k^y & 0 & 0 & 0 & 0 \\ c_1^z & c_2^z & \dots & c_k^z & 0 & 0 & 0 & 0 \end{bmatrix} \begin{bmatrix} d_1 \\ d_2 \\ \vdots \\ d_k \\ p_0 \\ p_1 \\ p_2 \\ p_3 \end{bmatrix} = \begin{bmatrix} h_1 \\ h_2 \\ \vdots \\ h_k \\ 0 \\ 0 \\ 0 \\ 0 \end{bmatrix} \tag{10}$$

Solving this we can get weights d_i. Substituting weights into the implicit function 8 and also employing iso-surface method, we generate a volume consisting of two initializations. The generated volume is intersected with slices in between. These intersections are used to initialize Metamorph models on those slices. Note that this step only generates iso-surface. For visualization, algorithms like marching cube are needed. During the deformation of Metamorph, volume can be reconstructed by calculating new weights d_j and substituting them into Formula 8. Finally 3D segmentation result is generated.

2.5. Volume Ratio

Using ASM's reference volume and Metamorph's 3D segmentation result, we can detect the topological changes of the brain (e.g., missing structures) based on the ratio of the two volumes:

$$VolumeRatio = \frac{V_{Metamorph}}{V_{ASM}} \tag{11}$$

If the structure is present, the ratio of the two volumes will be close to 1. If the structure is missing, ASM will produce mean shapes and hence mean reference volume, while Metamorph will segment a much smaller volume since there is no obvious pattern or boundary for two initializations to dilate. In this case, the ratio of the two volumes will be much less than 1. We can also compute the mean curvatures of Metamorph's results. Metamorph's irregular results usually have high curvatures, which indicate structure missing. Thus we can also predict structure missing solely from Metamorph's results. But considering ASM's reference volume and using volume ratio are more accurate. Comparing to the area based approach [16], volume provides more information and volume ratio is more stable. The results of the prediction method is discussed in the next section.

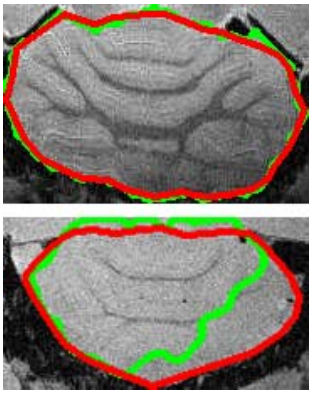

Figure 4. ASM and Metamorph's 2D results. Red lines represent ASM results, while green lines are Metamorph results. The top image shows normal case, while the bottom image is abnormal case (structure missing). Metamorph result is smaller in abnormal case. The difference is much larger in 3D.

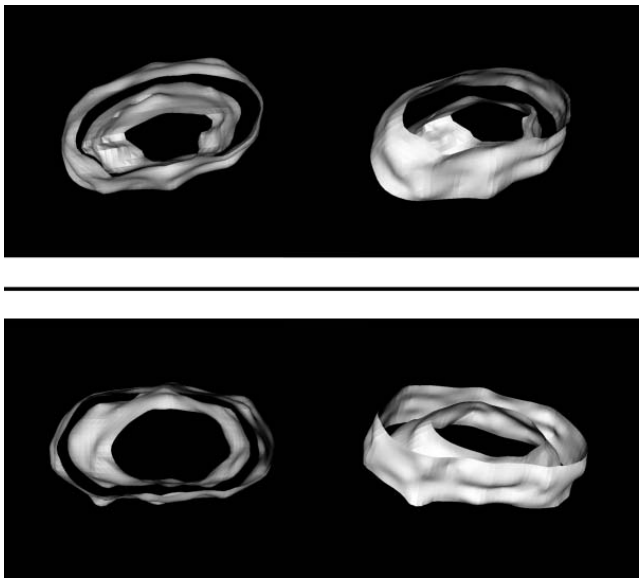

Figure 5. Metamorph's 3D segmentation results of 4 datasets (two normal cases and two abnormal cases). For better comparison and visualization, normal and abnormal cases are displayed together, and top as well as bottom parts are clipped. Each row represents two datasets (with different view ports in two columns). The outer shapes are results of normal structures, while the inner shapes come from abnormal cases (structure missing). The volume of inner shapes are much smaller than outer ones (less than one half). ASM's volumes are similar to Metamorph's results, which are not shown in this diagram.

3. Results

Four 4-month old female rats were anesthetized with chloral hydrate and transcardially perfused with PBS (0.1M, pH7.4), followed by 4% paraformaldehyde in PBS, using a PerfusionOne apparatus. The brains were left in the cranium to prevent distortions and damage and the heads were stored in 4% paraformaldehyde in PBS. The specimens were scanned on a 21T, 900MHz, Brucker Biospin MRI, with TE=5ms, TR=100ms, f.o.v. 3x2.16x2.58 and voxel size 0.06mm, isotropic. The MR images were seg-

mented with the use of the modeling and visualization package Amira 4.1 by experts to establish the ground truth.

To test the proposed detection method for the existence prediction of the cerebellum in the brain images, we generated 3000 training data, i.e., the image patches to be used in the nonparametric kernel regression. The data was obtained by randomly sampling 30 patches from each of 100 brain images that were randomly selected from the four rats brain MRI datasets discussed above. For the evaluation of the method, we selected 15 test datasets from the four rats brain MRI datasets which contains 8 datasets with the cerebellum and 7 datasets without the cerebellum.

In a test dataset, we randomly selected one image with the cerebellum and randomly scanned 50 positions to obtain 50 predictions for the target location. The result shows the majority of the prediction is close to the ground truth position although there are outliers.

We then segmented the testing brain datasets with and without the cerebellum using the RASM method slice by slice and 3D Metamorph models simultaneously, as described in Section 2.3 and 2.4, by initializing the models at the predicted locations. Top row of Fig. 4 shows the segmentation results of RASM of MR image of the brain slice by slice with cerebellum superimposed on the segmentation results of 3D Metamorph models. The results show that the volume segmented by ASM slice by slice and the volumes segmented by 3D Metamorph model are approximately the same and the ratio of the volumes is close to 1.

On the other hand, bottom row of Fig. 4 shows the segmentation results of RASM of MR image of the brain slice by slice without cerebellum superimposed on the segmentation results of 3D Metamorph models. The results show that the volume segmented by ASM is much larger than the volume segmented by Metamorph model due to the Metamorph's insufficient balloon force. The ratio of the volumes segmented by ASM slice by slice and the volumes segmented by Metamorph model is much large than 1.

The 3D Metamorph results of 4 datasets (out of 15) are shown in Fig. 5. 2 are normal cases and the others are abnormal. For a better comparison and visualization, normal and abnormal cases are displayed together. Top and bottom parts are clipped. Thus we can observe both cases at the same time. Each row represents two datasets, normal and abnormal, with different view ports in two columns. The outer shapes are results of normal structures, while the inner shapes come from abnormal cases (structure missing). The volume of inner shapes are much smaller than outer ones (less than one half). ASM's volume magnitude are similar to Metamorph's results, which are not shown in this diagram.

Out of 15 test datasets, there were 7 correct predictions of the cerebellum (out of 8) and 6 correct predictions of non-cerebellum (out of 7). Thus, there is a 86.6% success rate for detecting the cerebellum correctly. These promising results are summarized in Table 1. With the proposed method, we can address the issue of missing or emerging structures of interest, which many proposed methods require a priori knowledge to handle.

Table 1. Results of cerebellum prediction using structure prediction method.

	No cerebellum detected	Cerebellum detected
With Cerebellum	1	7
Without cerebellum	6	1

4. Conclusion

We proposed a novel method to detect and segment 3D brain structures by allowing the accurate initialization of deformable models. Combining ASM's reference volume, we can predict the existence of brain structures. The proposed method focused on the topological changes of brain structures including missing and emerging structures, based on a novel *volume ratio* criteria. With these promising results, the method can be used to provide a high throughput automatic segmentation of rodent brains for many different preclinical neuroscience applications.

References

[1] A. Pitiot, H. Delingette, and P. Thompson, *Medical Image Systems: Technology and Applications*, ch. Automated Image Segmentation: Issues and Applications. Academic Press, 2004.

[2] V. Boronikolas, M. Michaelides, J. Zhou, G. Wang, S. Blackband, S. Grant, D. Metaxas, N. Volkow, and P. Thanos, "Validation of the active shape model for automatic brain region segmentation," *IEEE Nuclear Science Symposium and Medical Imaging Conference*, 2006.

[3] R. McCarley, C. Wiblea, M. Frumina, Y. Hirayasua, J. Levitta, I. Fischera, and M. Shenton, "Mri anatomy of schizophrenia," *Biological Psychiatry*, vol. 45, no. 9, pp. 1099–1119, 1999.

[4] O. Carmichael, H. Aizenstein, S. Davis, J. Becker, P. Thompson, C. Meltzer, and Y. Liu, "Atlas-based hippocampus segmentation in alzheimer's disease and mild cognitive impairment," *NeuroImage*, vol. 27, no. 4, pp. 979–990, 2005.

[5] F. Delis, Y. Ma, H. Benvenste, D. Grandy, G. Wang, N. Volkow, and P. Thanos, "Effects of chronic alcohol intake and dopamine d2 receptor gene expression on brain anatomy: an in-vivo mri volumetric study of the mouse brain," in *Society for Neuroscience*, 2008.

[6] I. Rabkin, F. Delis, Y. Ma, S. Grant, G. Wang, N.D.Volkow, J. Shih, and P. Thanos, "Monoamine oxidase a gene knockout mouse brain anatomy:an in-vitro mri volumetric study," in *Society for Neuroscience*, 2008.

[7] A. Pitiot, H. Delingette, P. Thompson, and A. N., "Expert knowledge-guided segmentation system for brain mri," *NeuroImage*, vol. 23, pp. s85–s96, 2004.

[8] M. Leventon, E. Grimson, and O. Faugeras, "Statistical shape influence in geodesic active contours," *IEEE Proc. of Computer Vision and Pattern Recognition*, pp. 4–11, 2000.

[9] V. Barra and J. Boire, "Automatic segmentation of subcortical brain structures in mr images using information fusion," *IEEE transctions on medical imaging*, vol. 20, no. 7, pp. 549–558, 2001.

[10] W. Niessen, K. Vincken, J. Weickert, B. Romeny, and M. Viergever, "Multiscale segmentation of three-dimensional mr brain images," *International Journal of Computer Vision*, vol. 31, no. 2, pp. 185–202, 1999.

[11] D. Shen, E. Herskovies, and C. Davatzikos, "An adaptive-focus statistical shape model for segmentation and shape modeling of 3d brain structures," *IEEE Transactions on Medical Imaging*, vol. 20, no. 4, pp. 257–270, 2001.

[12] J. Zhou, S. Chang, Q. Liu, G. Pappas, V. Boronikolas, M. Michaelides, N. Volkow, P. Thanos, and D. Metaxas, "A novel learning based segmentation method for rodent brain structures using mri," *IEEE International Symposium on Biomedical Imaging: From Nano to Macro*, pp. 61–64, 2008.

[13] T. Cootes, C. Taylor, D. Cooper, and J. Graham, "Active shape models-their training and application," *Computer Vision and Image Understanding*, vol. 61, no. 1, pp. 38–59, 1995.

[14] X. Huang, D. Metaxas, and T. Chen, "Metamorphs: Deformable shape and texture models," in *IEEE Computer Society Conf. on Computer Vision and Pattern Recognition, CVPR*, 2004.

[15] X. Huang and D. Metaxas, "Metamorphs: Deformable shape and appearance models," *TPAMI*, vol. 30, no. 8, pp. 1444–1459, 2008.

[16] J. Zhou, S. Chang, S. Zhang, G. Pappas, M. Michaelides, F. Delis, N. Volkow, P. Thanos, and D. Metaxas, "Segmentation of rodent brains from mri based on a novel statistical structure prediction method," in *IEEE International Symposium on Bomedical Imaging (ISBI)*, 2009.

[17] G. Turk and J. F. O'Brien, "Shape transformation using variational implicit functions," in *The Proceedings of ACM SIGGRAPH 99*, pp. 335–342, 1999.

[18] T. Hastie, R. Tibshirani, and J. Friedman, *The Elements of Statistical Learning: Data Mining, Inference, and Prediction*. Springer-Verlag, New York, 2001.

[19] S. Zhou, J. Zhou, B. Georgescu, and D. Comaniciu, "A boosting regression approach to medical anatomy detection," *CVPR*, pp. 1–8, 2007.

[20] F. De La Torre and M. Black, "A framework for robust subspace learning," *International Journal of Computer Vision*, vol. 54, no. 1-3, pp. 117–142, 2003.